Topological Cathodes: Eliminating the Space Charge Limit of Electron Emission Using Metamaterials

David H. Dowell
SLAC and Seattle

Image charge and the space charge limit of cathodes

In high voltage RF and DC photocathode guns space charge limited emission occurs when the image charge field and the applied field are equal.

$$E_{applied} = \frac{Q}{\epsilon_0 \pi R^2}$$

For a metal-like cathode, the image charge is equal in magnitude but opposite in sign compared to the real charge. But if the cathode is a dielectric then the image-charge to real-charge ratio is given more generally by

$$\frac{q'}{q} = -\left(\frac{\epsilon_c - 1}{\epsilon_c + 1}\right)$$

Where ϵ_c is the cathode dielectric constant or relative electric permittivity defined in terms of the cathode's electric permittivity, $\epsilon_{cathode}$, and electric susceptibility, χ_e, as

$$\epsilon_{cathode} = \epsilon_0 \epsilon_c = \epsilon_0 (1 + \chi_e)$$

Usually, $|\epsilon_c| \gg 1$ which makes

$$\frac{q'}{q} = -1$$

However, as will be shown, ϵ_c and hence the image charge strongly depend upon frequency near the plasma frequency of the surface.

The Drude dielectric function for copper

In Drude's theory the dielectric function is specified in terms of the material's plasma frequency and relaxation time. For a metal the dielectric function is,

$$\epsilon(\omega) = 1 + \frac{\omega_p^2}{\omega\left(\omega + \frac{i}{\tau_p}\right)}$$

where the plasma frequency of the metal is given by the number density, n, of conduction band electrons: $\omega_p^2 = \frac{4\pi n e^2}{m}$

and the relaxation time, τ_p, depends upon the electrical conductivity, σ: $\tau_p = \frac{m\sigma}{ne^2}$

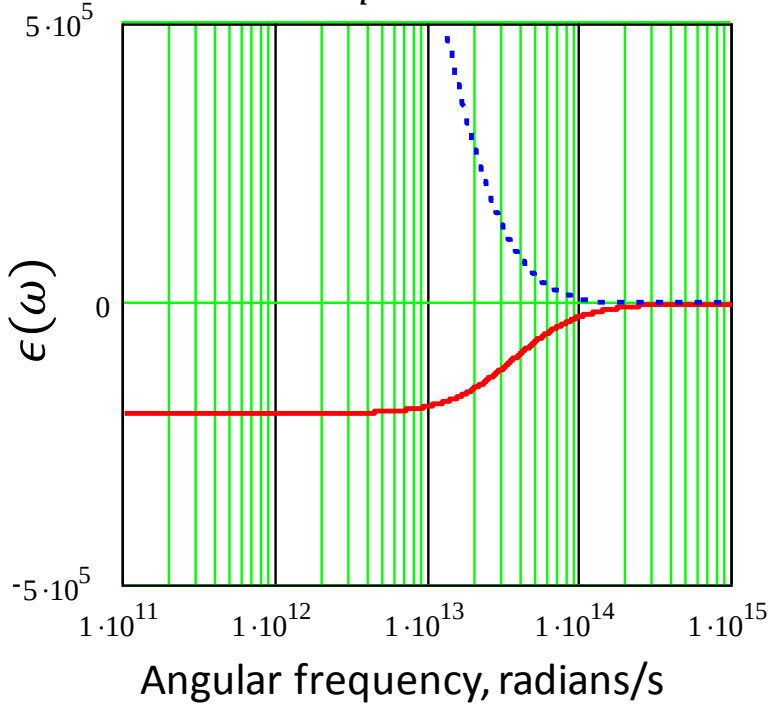

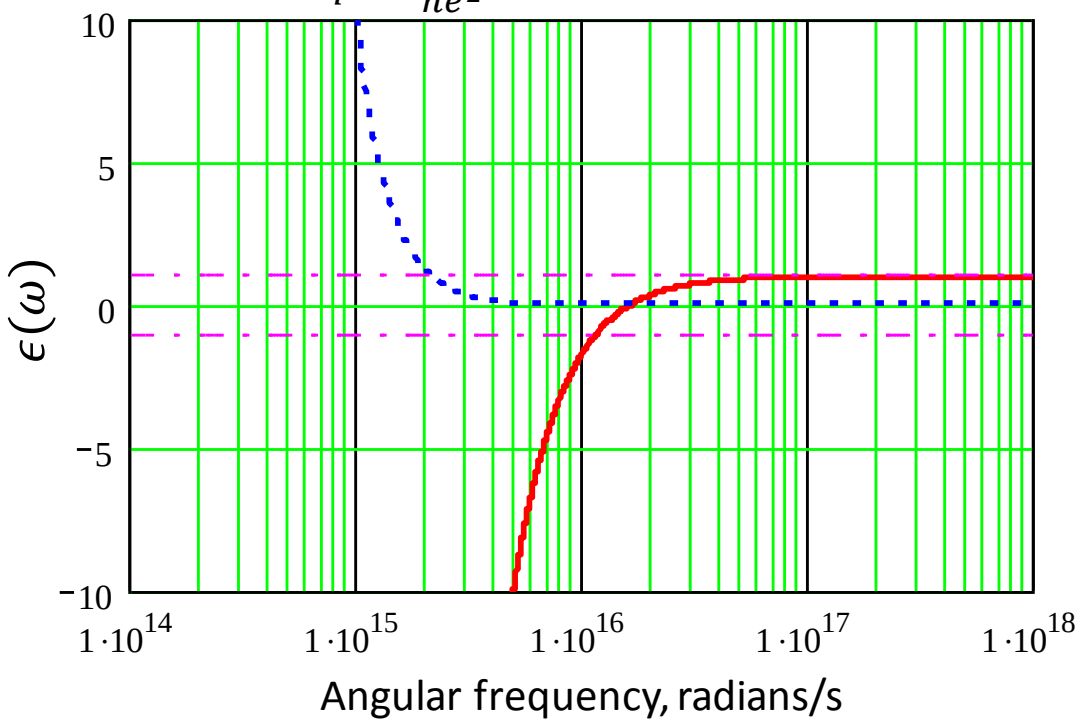

The complex dielectric function for copper at room temperature plotted with different vertical and horizontal scales. The real part is plotted with the solid-red curves and the imaginary part is plotted using dash-blue curves. The plasma frequency is 1.64x10^{16} rad/second and is the frequency where the real part is zero.

The Transition Frequency

The transition from metal to vacuum occurs when the denominator is zero, or when

$$\epsilon_c(\omega_t) = -1$$

Here ω_t is the transition frequency. Taking the real part of the Drude formulation for ϵ_c we have,

$$Re\left(1 + i\frac{\omega_p^2 \tau_p}{\omega_t(1 - i\omega_t \tau_p)}\right) = -1$$

Solving for ω_t gives $\omega_t = \sqrt{\frac{\omega_p^2}{2} - \frac{1}{{\tau_p}^2}}$

$$\frac{q'}{q} = -\left(\frac{\epsilon_c(\omega) - 1}{\epsilon_c(\omega) + 1}\right)$$

The image-charge-to-real-charge ratio as a function of frequency for copper. The blue curve is the imaginary part and the red curve is the real part. A dash-dot line is drawn at -1 corresponding the charge ratio assumed in current cathode models. The transition frequency is ω_t=1.16x10^{16} radians/second.

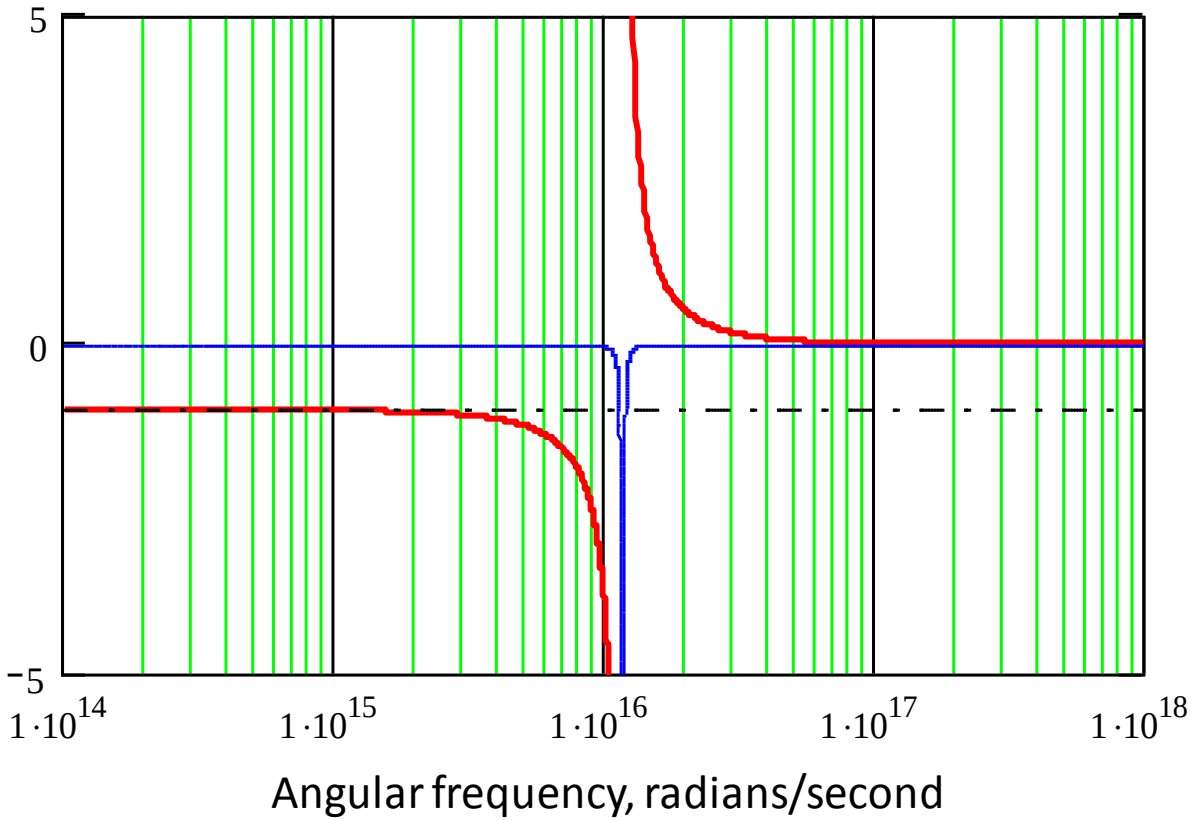

Image-Charge Fields at the Cathode Surface

The image method places an image of the real charge at the symmetrical position on the inside of the cathode to calculate the field it produces on the outside the cathode. The Figure shows the image method's configuration for a real-charge disk at $z=z_s$ and its image is at $-z_s$. When $z_s = 0$ the disk is at the cathode surface. The first term is the potential energy of the applied field.

$$V_{total}(z_s) = -E_a z_s - \frac{Q_0}{\epsilon_0 \pi R^2}\left(\frac{\epsilon_c - 1}{\epsilon_c + 1}\right)\left(\sqrt{z_s^2 + \frac{R^2}{4}} - z_s\right)$$

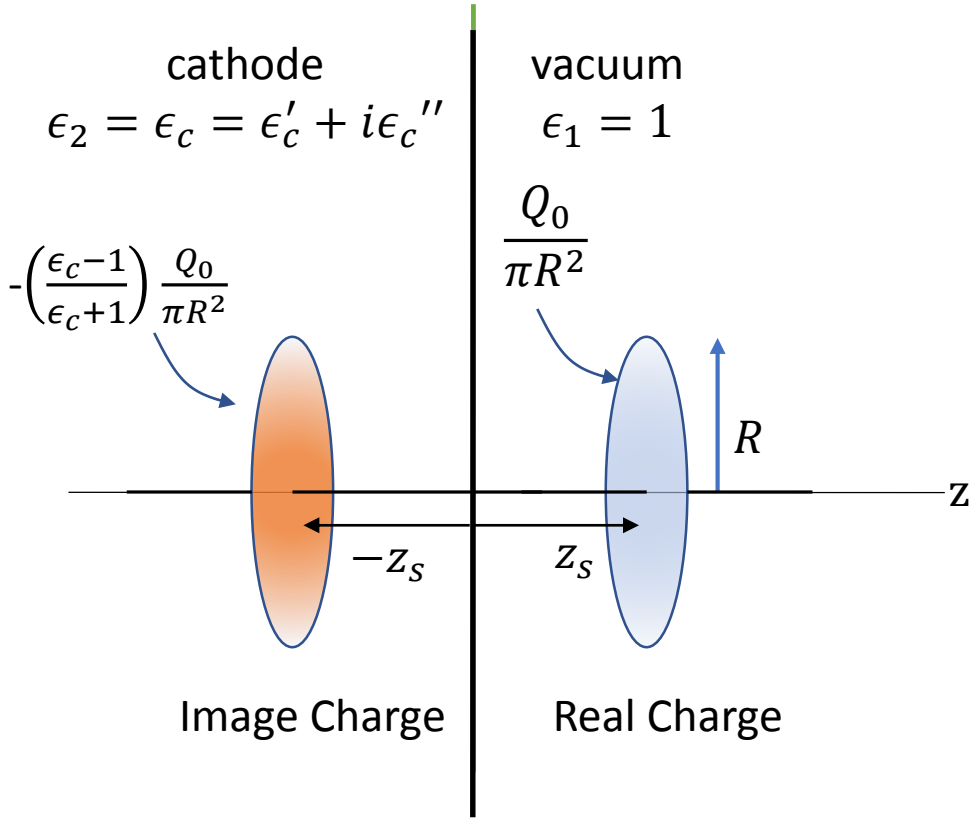

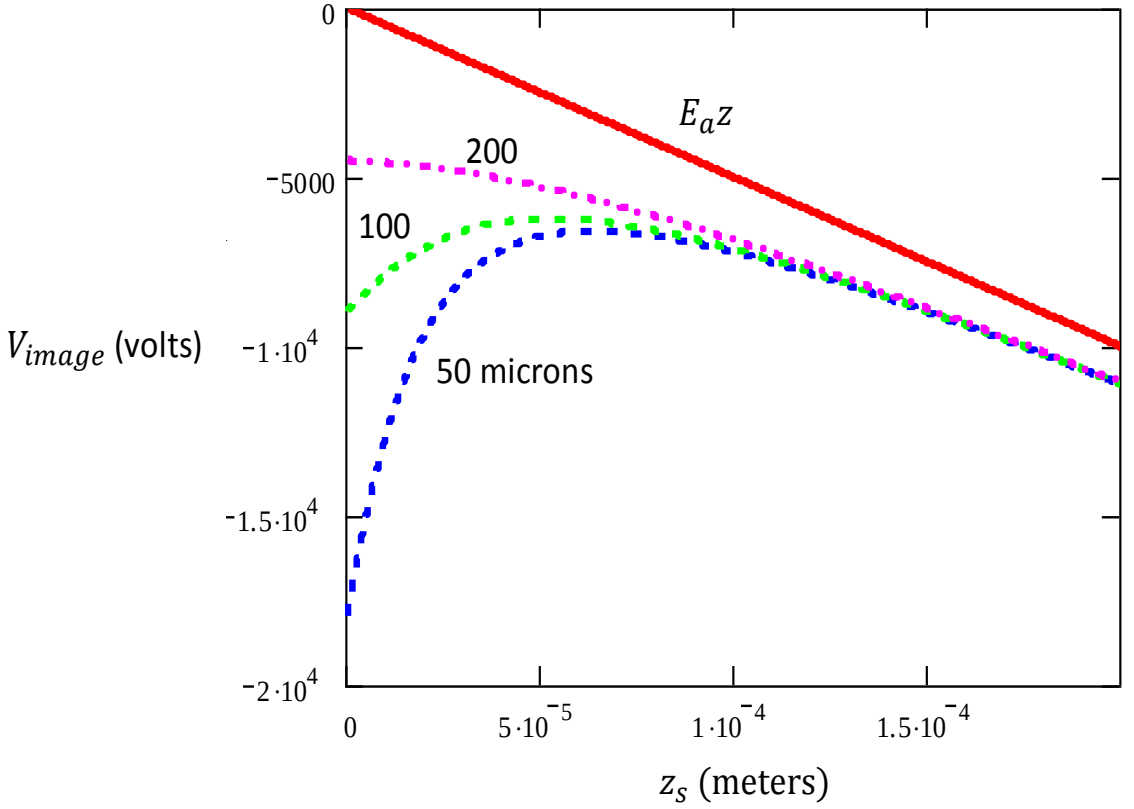

The Electric Field of the Image Charge at the Center of the Accelerating Disk

$$\vec{E}_{image} = -\vec{\nabla}V_{image} \quad \rightarrow \quad E_{image}(z(t)) = \frac{Q_0}{\epsilon_0 \pi R^2}\left(\frac{\epsilon_c - 1}{\epsilon_c + 1}\right)\left(\frac{z(t)}{\sqrt{z(t)^2 + \frac{R^2}{4}}} - 1\right)$$

For acceleration from rest: $z(t) = \frac{1}{\gamma'}\left(\sqrt{(\gamma' ct)^2 + 1} - 1\right)$ and $\gamma' \equiv \frac{E_{applied}}{mc^2}$

Fitting the width and amplitude of a Gaussian to E_{image} gives the following useful formula,

$$E_{image}^{gaussian}(t) = -\frac{Q_0}{\epsilon_0 \pi R^2}\left(\frac{\epsilon_c - 1}{\epsilon_c + 1}\right) e^{-\frac{t^2}{2\sigma_t^2}}$$

The rms width of the gaussian is a function of the disk radius and the normalized applied field,

$$\sigma_t^2 \equiv \frac{\left(1 + \gamma' R/\sqrt{12}\right)^2 - 1}{2 \ln 2 \, \gamma'^2 c^2}$$

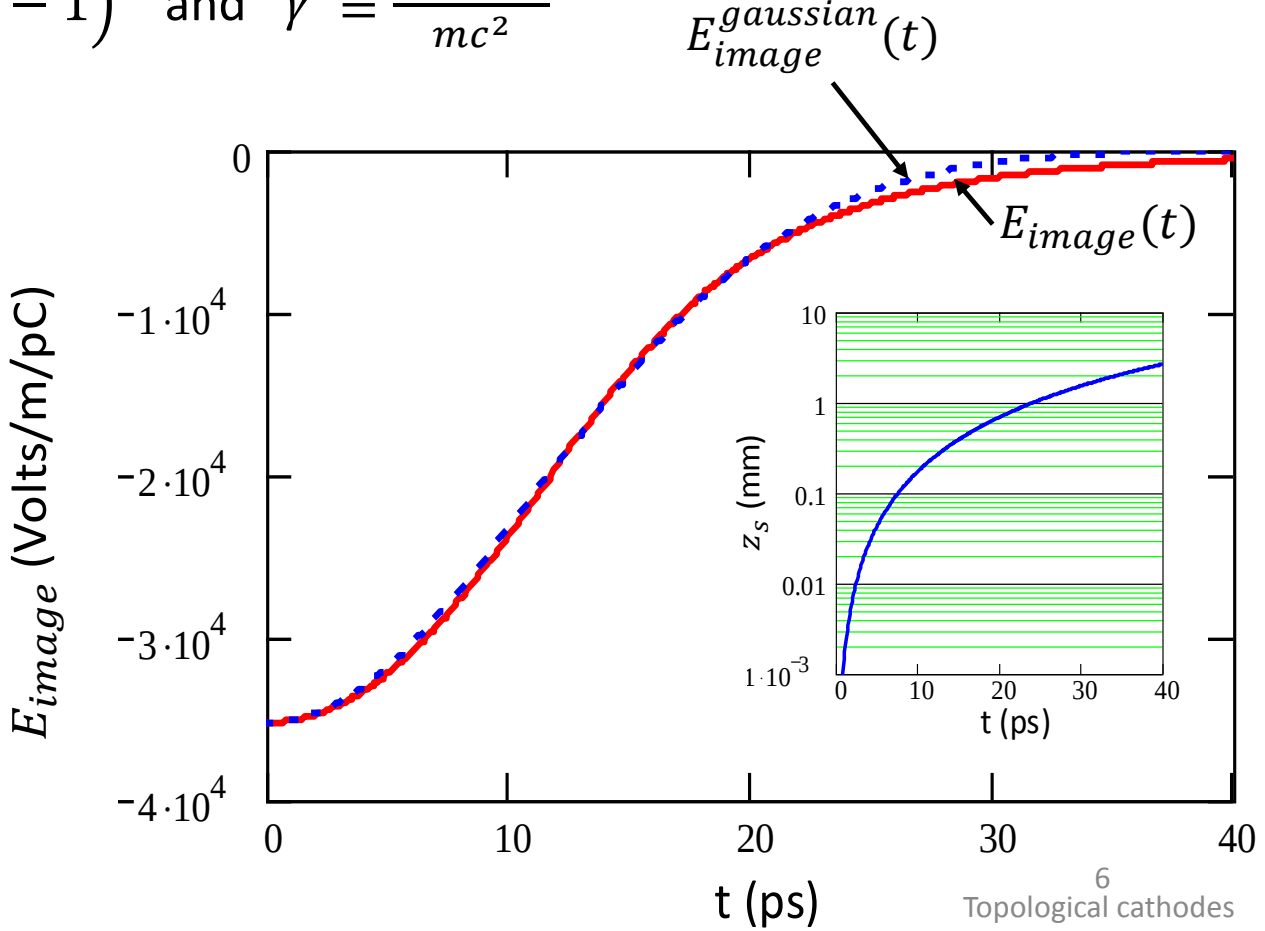

Fourier transforms of the image-charge field

The Fourier integral is used to obtain the frequency spectrum of the time-dependent field seen by the disk as it accelerates from the cathode. This spectrum is a source of changing fields which drives currents in the cathode to produce the image charge via the frequency response of the dielectric function.

Since the function $E_{image}(t)$ is an even function in time the image field is given by the following

$$\tilde{E}_{image}(t) = \int_0^\infty A_{image}(\omega)\cos\omega t\, d\omega \tag{20}$$

Where

$$A_{image}(\omega) = \frac{2}{\pi}\int_0^\infty E_{image}(t)\cos\omega t\, dt \tag{21}$$

$A_{image}(\omega)$ is the frequency spectrum of the image-charge field see by the disk as it accelerates from the cathode. Assuming the gaussian formulation for the image-charge field, the integral in Eqn. (21) is easily computed with the result

$$A_{image}^{gaussian}(\omega) = -\sqrt{\frac{2}{\pi}}\frac{Q_0}{\epsilon_0\pi R^2}\left(\frac{\epsilon_c(\omega)-1}{\epsilon_c(\omega)+1}\right)\sigma_t e^{-\frac{\omega^2\sigma_t^2}{2}} \tag{22}$$

This expression gives the frequency spectrum of the image-charge field responding to the electrical impulse generated by the accelerating disk. Transforming this spectrum back to time gives

$$\tilde{E}_{image}^{gaussian}(t) = -\sqrt{\frac{2}{\pi}}\frac{Q_0}{\epsilon_0\pi R^2}\sigma_t\int_0^\infty\left(\frac{\epsilon_c(\omega)-1}{\epsilon_c(\omega)+1}\right)e^{-\frac{\omega^2\sigma_t^2}{2}}\cos\omega t\, d\omega \tag{23}$$

Using Drude's theory for the dielectric function this expression can be written in terms of the plasma frequency and the decay time of the cathode surface,

$$\tilde{E}_{image}^{gaussian}(t) = -\sqrt{\frac{2}{\pi}}\frac{Q_0}{\epsilon_0\pi R^2}\sigma_t\int_0^\infty\left(\frac{\omega_p^2}{\omega_p^2-2\omega\left(\omega+\frac{i}{\tau_p}\right)}\right)e^{-\frac{\omega^2\sigma_t^2}{2}}\cos\omega t\, d\omega \tag{24}$$

The dielectric function of a meta-surface: Image-charge field as a function of the transition frequency

An example of a meta-surface is a rectangular array of vertical, metallic wires standing above the cathode surface. Such an array has a plasma frequency given by

$$\omega_{wire}^2 = \frac{2\pi c^2}{a^2 \ln\frac{a}{r}} \tag{25}$$

and the relaxation time is

$$\tau_{wire} = \frac{r^2 \sigma_{wire}}{2\epsilon_0 c^2} \ln\frac{a}{r} \tag{26}$$

Here a is the center-to-center distance between the wire, r is the wire radius, and c is the speed of light. The conductivity of each wire is σ_{wire}, and ϵ_0 is the permittivity of the vacuum between the wires.

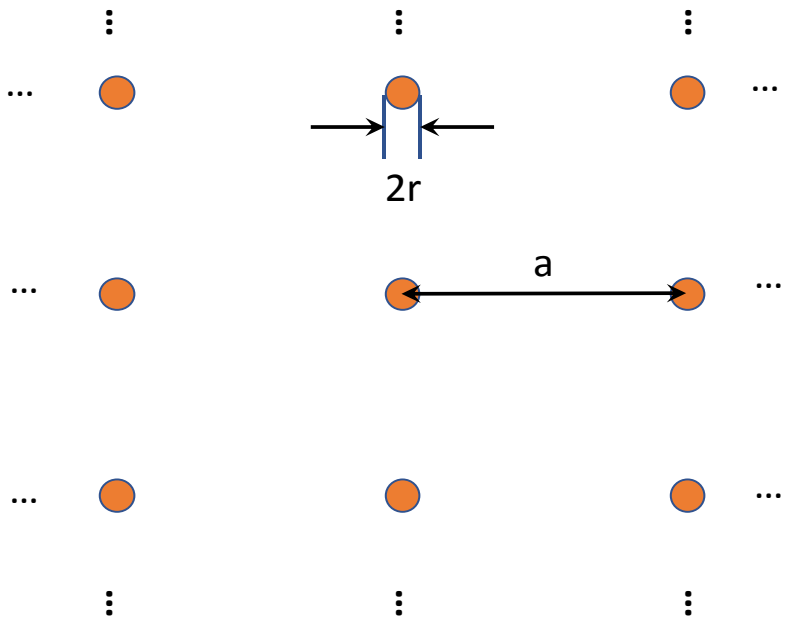

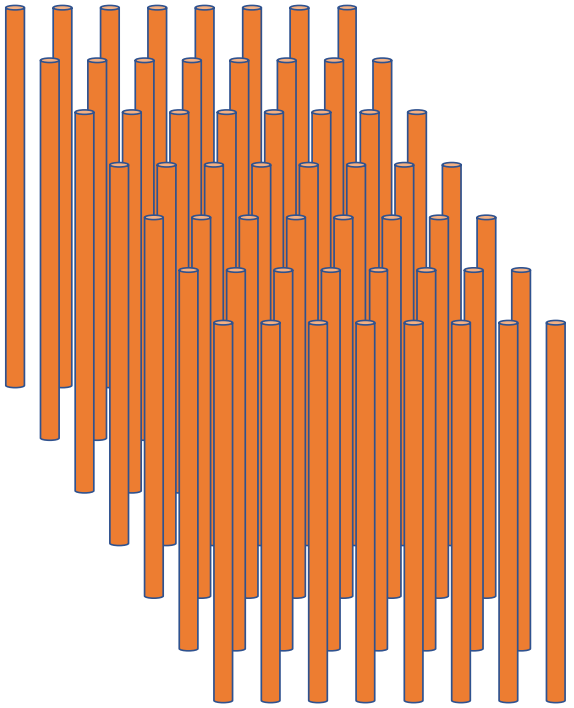

Response of metasurfaces with transition frequencies above, near and below the beam spectrum

Parameter			
wire spacing, a (mm)	0.1	1	10
wire radius, r (microns)	10	10	10
wire conductivity, σ_{wire}	6.3×10^{5}	6.3×10^{5}	6.3×10^{5}
relaxation time, τ_{wire} (sec)	9.1×10^{-11}	1.8×10^{-10}	2.7×10^{-10}
array plasma freq., ω_{wire} (radians/sec)	4.9×10^{12}	3.5×10^{11}	2.9×10^{10}
transition frequency, ω_t (radians/sec)	3.5×10^{12}	2.5×10^{11}	2.0×10^{10}

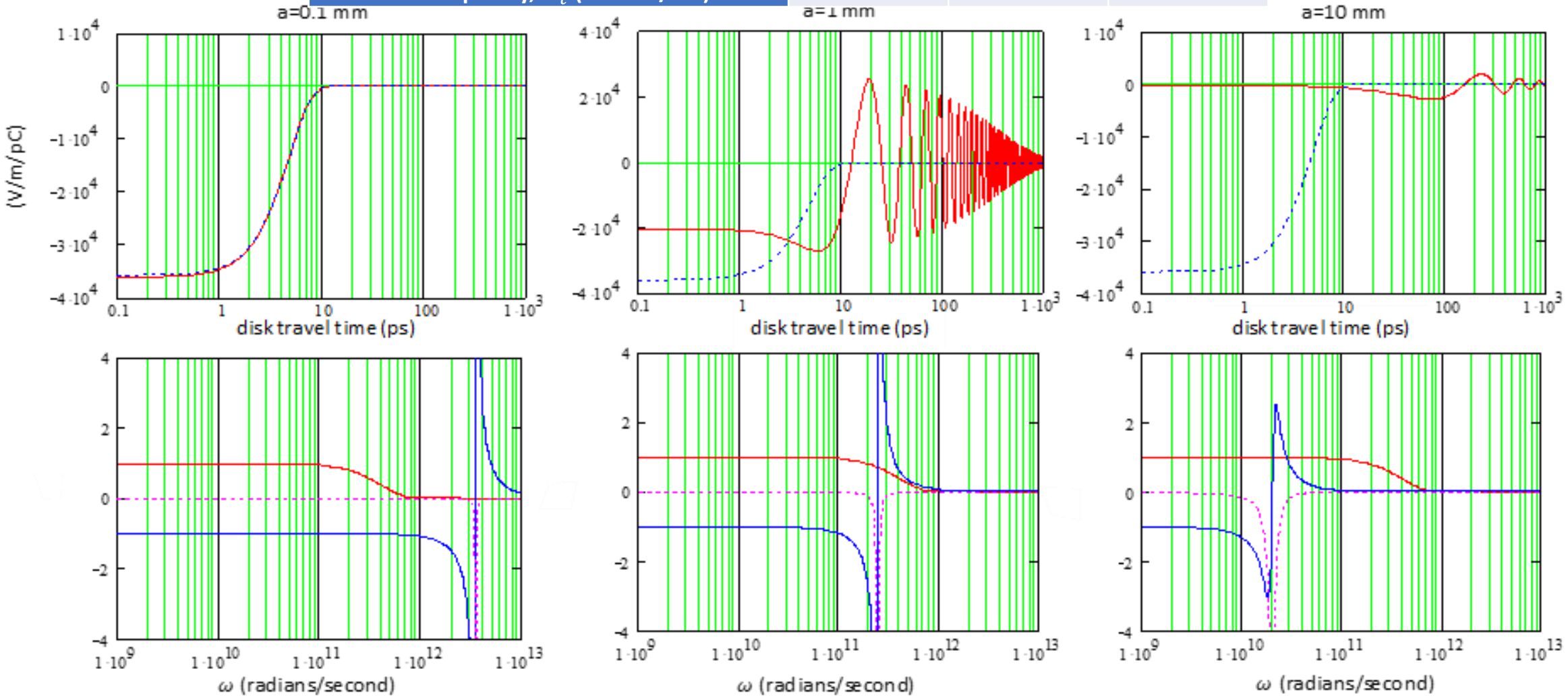

An optimized wire-array metamaterial for cancelling the space-charge limit

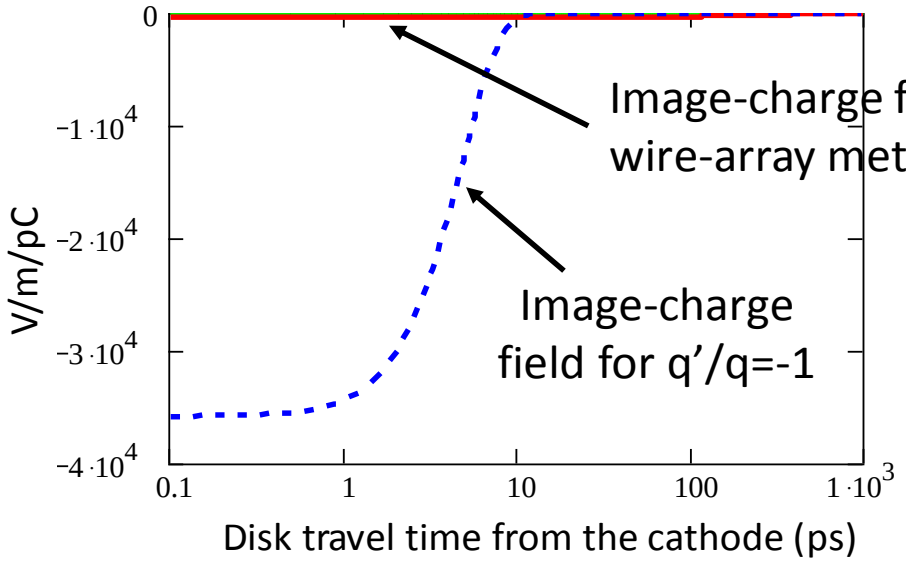

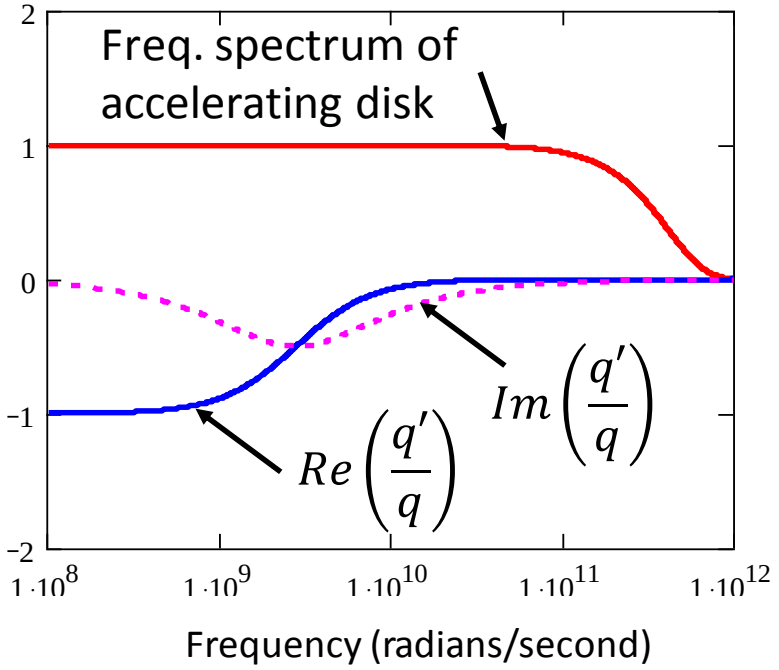

Parameters for rectangular array of vertical wires. The wire conductivity is 1/1000 that of copper.

Parameter	Value
wire spacing, a (mm)	0.2
wire radius, r (microns)	0.1
wire conductivity, σ_{wire} (S/m)	$6.3\text{x}10^{4}$
relaxation time, τ_{wire} (sec)	$3.0\text{x}10^{-15}$
minimum wire length (microns)	1
array plasma freq., ω_{wire} (radians/sec)	$1.4\text{x}10^{12}$
transition frequency, ω_t (radians/sec)	$3.3\text{i x}10^{14}$

Figure Top: The image-charge electric field at the disk center as a function of the disk's time of travel. The dash-blue curve is the field with q'/q=-1 and the solid-red curve is the field with an array of wires with the parameters given in the Table.

Bottom: The frequency spectrum of the accelerating disk is shown with a solid-red curve. The real (solid-blue) and imaginary (dash-magenta) q'/q as a function of frequency or the negative of the surface response function, $\frac{q'}{q} = -g_c(\omega)$.The disk radius is R= 1 mm and the normalized applied field is $\gamma' = 39$ /m.

The transverse size of the metasurface can be estimated from the disk's position when the image-charge field decays to zero

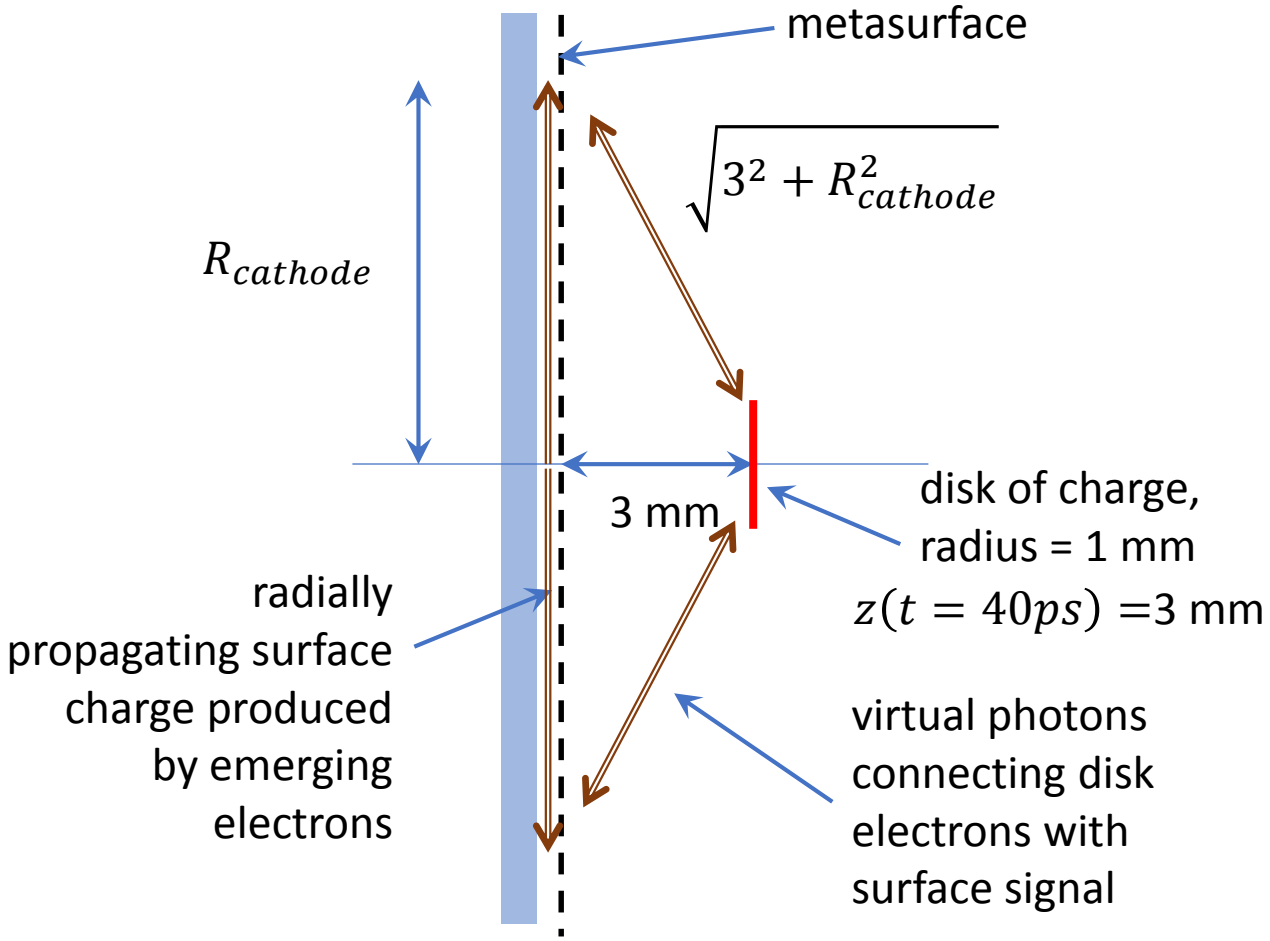

The time it takes a signal to travel from center to edge of cathode and back to disk should longer than the time it takes the image-charge field to decay. That way the signal dies away before the disk can know about the cathode's finite radius. In our example, if the signal velocity is c, then the round-trip distance needs to be longer than the distance light travels in 40 ps, or $ct = 12mm$. Therefore

$$R_{cathode} + \sqrt{3^2 + R_{cathode}^2} \geq 12\,mm$$

$$\therefore R_{cathode} \geq 6\,mm$$

Length of the wires

Although the wire-array model assumes the wires are isolated, for the metasurface this condition is severely violated since one end is electrically connected to the cathode surface. However, the assumption can be made valid provided the wires are long enough that a signal sent from the free end decays before reaching the attached end. In this case, the wires appear to be infinitely long.

Since the fastest any signal can travel is the speed of light, the wire should be longer than $c\,\tau_{wire}$.

The relaxation times for the first set of meta surfaces are all very long which lead to values of $c\,\tau_{wire}$ which are several mm long:

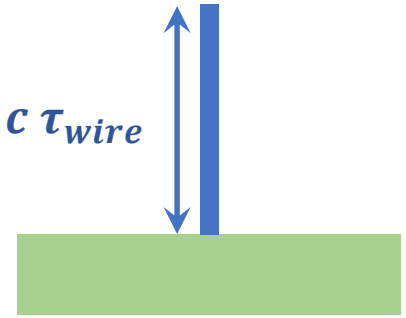

Parameter			
wire spacing, a (mm)	0.1	1	10
wire radius, r (microns)	10	10	10
wire conductivity, σ_{wire}	$6.3\text{x}10^{5}$	$6.3\text{x}10^{5}$	$6.3\text{x}10^{5}$
relaxation time, τ_{wire} (sec)	$9.1\text{x}10^{-11}$	$1.8\text{x}10^{-10}$	$2.7\text{x}10^{-10}$
array plasma freq., ω_{wire} (radians/sec)	$4.9\text{x}10^{12}$	$3.5\text{x}10^{11}$	$2.9\text{x}10^{10}$
transition frequency, ω_t (radians/sec)	$3.5\text{x}10^{12}$	$2.5\text{x}10^{11}$	$2.0\text{x}10^{10}$
minimum wire length, $c\,\tau_{wire}$ (mm)	27	54	81

However, the relaxation time is much shorter for the optimized wire-array giving a more practical minimum wire length of one micron.

Parameter	Value
wire spacing, a (mm)	0.2
wire radius, r (microns)	0.1
wire conductivity, σ_{wire} (S/m)	$6.3\text{x}10^{4}$
relaxation time, τ_{wire} (sec)	$3.0\text{x}10^{-15}$
array plasma freq., ω_{wire} (radians/sec)	$1.4\text{x}10^{12}$
transition frequency, ω_t (radians/sec)	$3.3\text{i x}10^{14}$
minimum wire length, $c\,\tau_{wire}$ (microns)	0.9

RF Heating and Skin Depth

The RF skin depth is given by $\delta = \sqrt{\frac{2}{\mu_c \omega \sigma}}$

The RF frequency is $\omega = 2\pi f_{RF}$, the conductor's permeability is μ_c and its conductivity is σ.

5 micron long wires, $\delta_{meta} = 147$ microns

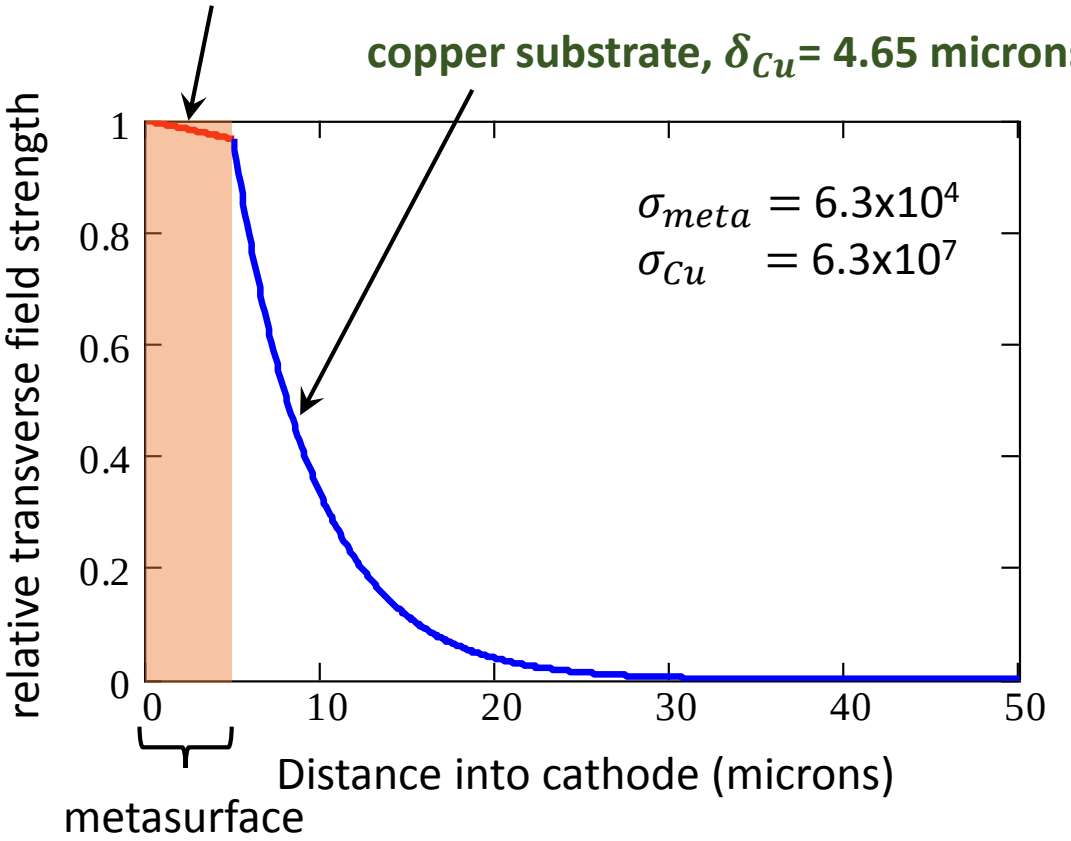

As an example, assume the LCLS-II RF gun frequency of 186 MHz. Using the $6.3\text{x}10^4$ S/m conductivity of the optimized wire array gives a skin depth of 147 microns. Thus, the RF passes through the 1-micron tall wire array with little dissipation with most of the power being deposited in the higher conductivity metal below with a much shorter skin depth of 4.65 microns.

Problems and issues hindering the use of meta-surfaces in high field guns

Another possible heat source is the current of the beam itself as it is drawn from the surface. Here the heating can be mitigated by designing the emission area to be between the wires, and not from the wires themselves. **Since the wire spacing is 200 microns, a small region four or five wires in diameter could be designated as an emission area. The effect of the 'defect' in this regular lattice of wires on the overall dielectric function can be studied, and the array properties modified near the defect to mitigate any detrimental effects it may have on the surface response function.** In cathodes using field emission from points, needles or other high-aspect shapes, individual low conductivity wires can be replaced by one or several field-emission points.

An important issue is the electrical breakdown of any high-aspect metasurface with a high applied field. This phenomenon requires serious study, **the low conductivity wires could have high dissipative losses and in fact will burnup if they draw too much current**. This most certainly will occur during high-field arcing and RF processing. Another concern is multipacting which may occur between the wires and other surfaces. These and other effects require further theoretical and experimental study. To remedy these effects other meta-surface designs with a low profile such as split-ring resonators should be investigated.

Another metasurface is Pendry's dual split-ring resonator.

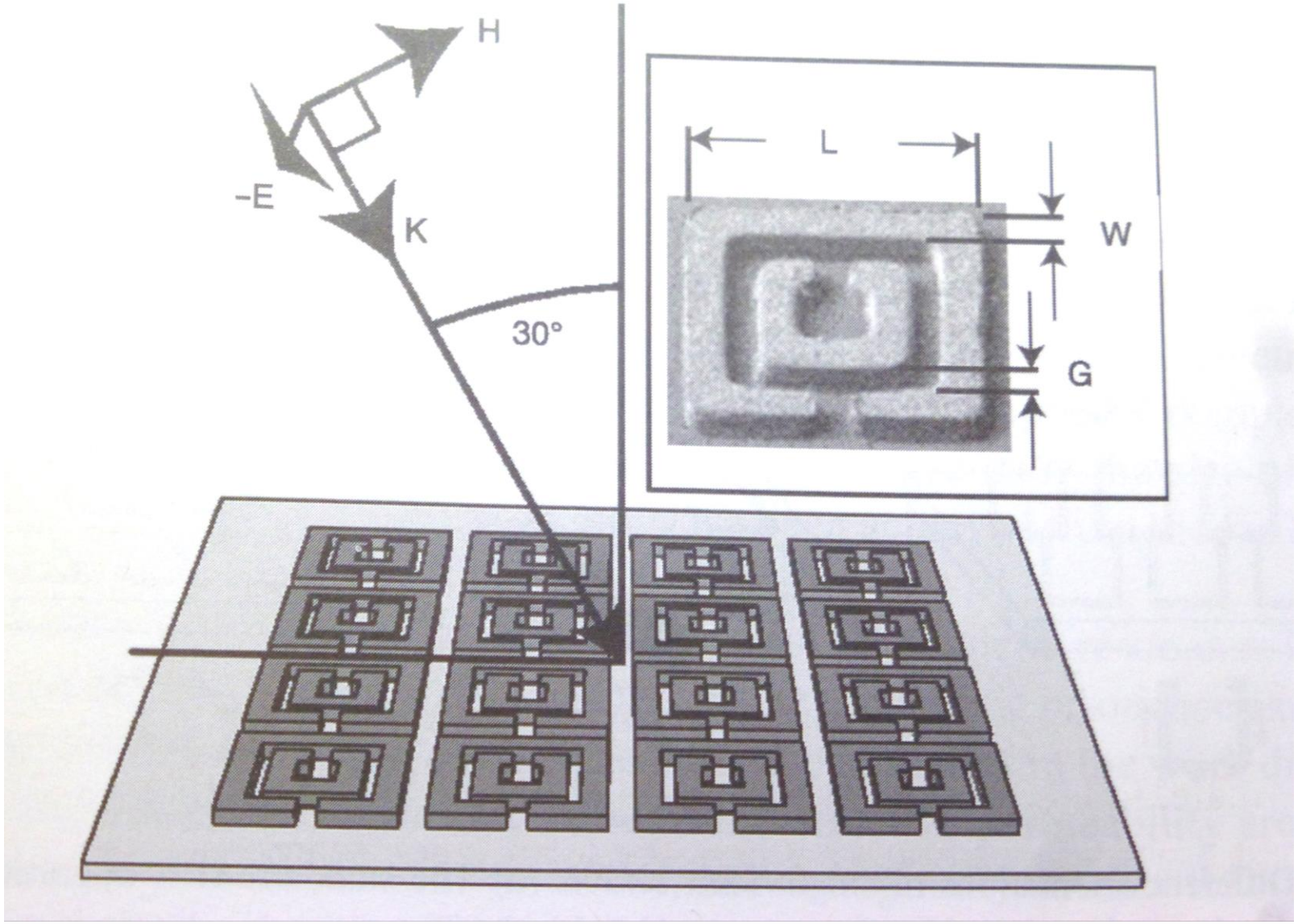

Pendry et al.

Summary and Conclusions

A theory for the response of a cathode to an emitted disk of charge was given in detail. This theory was then applied to Drude models for wire-array metasurfaces with transition frequencies around the accelerating disk's image-charge field frequency spectrum. Strong oscillations are seen when the transition frequency overlaps the high frequency edge of the disk's spectrum.

It was shown that a single set of wire-array parameters can found which completely eliminates the space charge limit at all charges and all applied fields.

The wire-array metasurface discussed in this paper is intended to demonstrate the concept of space charge control via a cathode's dielectric function. Other more sophisticated meta-structures like split ring resonators should also be investigated for the array atoms.

Future research should explore the use of topological surfaces to control electron emission in both RF and DC guns with both photoelectric and thermionic cathodes. This work opens new possibilities for electron source research with direct applications in accelerator physics.